



Aerosols drive monsoon rainfall spatial modulations over the Indian subcontinent: anthropogenic and dust aerosols impact, mechanism, and control

Sauvik Santra ¹, Shubha Verma ¹, Shubham Patel ¹, Olivier Boucher ², and Mathew Koll Roxy ³

¹Department of Civil Engineering, Indian Institute of Technology Kharagpur, Kharagpur, India

²Institut Pierre-Simon Laplace, Sorbonne Université / Centre National de la Recherche Scientifique, Paris, France

³Centre for Climate Change Research, Indian Institute of Tropical Meteorology Pune, Pune, India

Correspondence: Shubha Verma (shubha@iitkgp.ac.in)

Abstract. Spatial modulations in monsoon rainfall over the Indian subcontinent, characterized by persistent weakening and strengthening patterns, are yet to be understood in the context of the role of spatial heterogeneity in aerosol species (anthropogenic and dust) radiative perturbations, driving mechanism and control. Current inaccuracies in modelling the aerosol species burden in this region have posed challenges to fully addressing these complexities. Here, we successfully simulate for the first time the aerosol-driven impact on monsoon rainfall spatial modulations adequately accounting for aerosol distributions in a fine-resolved ($25 \times 25 \text{ km}^2$) regional climate model. The modelled aerosol-induced spatial modulations align consistently with the measured departures in monsoon rainfall. The aerosol-induced weakening of the rainfall (30%–50%) over most of the Indian subcontinent, with a maximum deficiency over the eastern coast (-48 mm), is primarily driven by changes in regional wind dynamics induced by anthropogenic aerosol all-sky radiative forcing. The rainfall increase ($> 50\%$) is strengthened by all-sky radiative warming with dust aerosols over most of central/northwestern India/western coast. Abatement of anthropogenic aerosols can largely mitigate the rainfall deficiency, but by 30% to 40% only over the eastern coast; thereby also identifying areas of augmented rainfall excessiveness (e.g. Andhra Pradesh/Gujarat) or their mitigation (e.g. Kerala/northeastern India) driven by anthropogenic aerosol control. These insights are crucial for developing effective water management strategies in the region.

1 Introduction

The Indian summer monsoon, which consists of monsoon rainfall occurring from June to September, is a crucial climatic phenomenon. It contributes over three-quarters of the annual rainfall across the Indian subcontinent (Parthasarathy et al., 1994; Ghosh et al., 2016; Rajendran et al., 2022). As a result, changes in the spatial and temporal variability of monsoon rainfall, as well as anomalies in the rainfall patterns, significantly impact water resources, agricultural production, and overall economic and societal prosperity. This, in turn, affects the quality of life for a large portion of the world's population in the Indian subcontinent (Lobell et al., 2011; Auffhammer et al., 2012; Skliris et al., 2022). Observational studies on monsoon rainfall over the Indian subcontinent report an increasing trend in heavy to extremely heavy rainfall events, notably in the central,



northwestern, and southernmost tip (Kerala region) of the Indian subcontinent (Rajesh and Goswami, 2023; Kripalani et al., 2022; Persad et al., 2022; Katzenberger et al., 2021; Zhang, 2020; Roxy et al., 2017). Additionally, some studies report a reduction in the monsoon rainfall over most of the northern and eastern Indo-Gangetic Plain (IGP) in the recent decades (2000 to 2018), negatively impacting groundwater levels and crop productivity in India (Seth et al., 2019).

The interannual variability of monsoon rainfall and the observed extreme rainfall events over south Asia is primarily linked to changes in global climatic patterns and the effects of greenhouse gases induced global warming in current studies (e.g. (Rajesh and Goswami, 2023; Singh et al., 2017; Roxy et al., 2017)). However, there are unexplained persistent regional spatial modulations (see Figure 1a), which include both strengthening and weakening trends in measured monsoon rainfall from the Indian Meteorological Department (IMD) (IMD-rainfall: June to September averaged rainfall from IMD measurements (2000–2019)). The observed spatial modulations in the measured monsoon rainfall do not seem to align with the effects of global warming due to greenhouse gases. Notably, the regions experiencing heavy rainfall events and those undergoing a decline in monsoon rainfall correspond with the areas identified in these regional spatial modulations. The mechanisms underlying these persistent spatial modulations in measured monsoon rainfall, particularly concerning the influence of spatially varying regional aerosols, have not yet been adequately addressed in the existing literature (Menon et al., 2002; Ramanathan et al., 2005; Bollasina et al., 2011; Vinoj et al., 2014; Samset et al., 2019; Persad et al., 2022; Christidis and Stott, 2022; Shawki et al., 2018; Risser et al., 2024; Stier et al., 2024).

Aerosol-monsoon interactions are influenced by the direct and indirect radiative effects of aerosols (Forster et al., 2007; Bollasina et al., 2011; Ganguly et al., 2012a; Sajani et al., 2012; Wang et al., 2017; Liou, 1980; Lawrence and Lelieveld, 2010). The direct radiative effect occurs when aerosols absorb and scatter solar radiation, leading to a reduction in surface insolation. This reduction can alter regional climate by lowering surface temperatures, enhancing atmospheric stability, and weakening winds and atmospheric circulations, which can trigger a response in the monsoon. Additionally, anthropogenic aerosol emissions can produce significant indirect effects by altering cloud characteristics (Charlson et al., 1992; Boucher and Lohmann, 1995; Eichel et al., 1996). This includes reducing cloud droplet size and enhancing cloud reflectivity, as well as increasing cloud lifetime and lowering precipitation efficiency. These changes impact the Earth's atmospheric radiative balance. The indirect effects of aerosols are particularly important during the summer monsoon season because the levels of liquid water content and moisture in the atmosphere are markedly higher during the season.

A clearer understanding of how aerosols impact the Indian monsoon is emerging from previous studies (Samset et al., 2019). For instance, the elevated heat (known as the elevated heat pump effect) caused by aerosols over the Tibetan Plateau is thought to enhance the meridional temperature gradient, which strengthens the early monsoon and influences its subsequent development (Lau et al., 2006). Additionally, dust-induced atmospheric heating over West Asia is believed to increase the flow of moisture into India and rapidly modulate monsoon rainfall over central India (Vinoj et al., 2014). Furthermore, absorbing aerosols is suspected to have a coincidental impact on monsoon breaks (Dave et al., 2017) and play a significant role in stabilizing the atmosphere through rapid adjustments that limit rainfall (Persad et al., 2022). However, there are still several limitations in our understanding of these interactions. It is necessary to examine the interactions between regional aerosols and the monsoon over the Indian subcontinent in context of the measured spatial modulations in the monsoon rainfall, particularly



delineating the role of regional anthropogenic aerosols relative to natural (e.g. desert dust) and greenhouse warming. This distinction is crucial because, unlike greenhouse gases, which are long-lived and contribute to global warming effects that are uniformly distributed across the globe, aerosols are primarily concentrated near their emission sources. Thus, they can exert a strong regional impact (Herbert et al., 2021). Moreover, anthropogenic and dust aerosols with distinct properties display significant spatial heterogeneity in their distribution across the Indian region (refer to Figure 1c-d, discussed later). This heterogeneity can lead to complex regional climatic interactions induced by aerosols (Boucher et al., 2016). Current inaccuracies in modelling the burden of aerosol species (both anthropogenic and dust) over the Indian region, as well as in accounting for their radiative effects in aerosol-climate models, have impeded our understanding of their interactions with the monsoon (Jin et al., 2016; Lau et al., 2017; Fadnavis et al., 2017; Barman and Gokhale, 2023; Debnath et al., 2023; Asutosh and Vinoj, 2024). These inaccuracies have also hindered efforts to validate the modelled aerosol-induced changes in rainfall with the observed rainfall deviations, thus necessitating scientific attention. Additionally, the coarse resolution of global aerosol-climate models, which are typically used in studies on aerosol-monsoon interactions, is insufficient for capturing the aerosol-induced changes in wind patterns, atmospheric circulation, and rainfall microphysical variables (Lau et al., 2017; Gadgil and Sajani, 1998; Cherian et al., 2013; Fadnavis et al., 2017). These factors are crucial for understanding how aerosols influence monsoon dynamics and the spatial patterns of monsoon-related rainfall (Lau et al., 2017; Gadgil and Sajani, 1998; Cherian et al., 2013; Fadnavis et al., 2017).

Here, we examine spatial modulations (weakening and strengthening) persistent in the measured monsoon rainfall over the Indian subcontinent in the context of spatial heterogeneity in regional aerosol species (anthropogenic and dust) radiative perturbations, driving mechanism and control. The assessment is done by designing an integrated modelling framework (see Figure S1 in the Supplementary Information) comprising aerosol response simulations (ARS) adequately accounting for regional aerosol distributions in a fine-resolved ($25 \times 25 \text{ km}^2$) weather research and forecasting (WRF) regional climate model. In conjunction, the available long-term (1901 to 2014) simulations of monsoon rainfall from a global aerosol climate model (IPSLCM6A-LR) in Climate Model Intercomparison Project Phase 6 (CMIP6) experiments (Boucher et al., 2020) are evaluated to delineate the role of aerosols relative to global greenhouse warming in driving the regional spatial modulations in the monsoon rainfall. Simulating the aerosols-driven role in monsoon rainfall spatial modulations over the Indian subcontinent is necessary to examine the implications of anthropogenic emissions and their mitigation on the required water management measures as presented in this study. Incorporating the above-mentioned implications in regulating water management is helpful in reducing the associated societal risks of rainfall deficiency and enhancement (e.g. flood risks) impacting the quality of life of one of the most populous regions in the world.

2 Methodology

The flowchart showing the methodology is presented in the Supplementary Information (Figure S1). We first analyse the spatially gridded ($25 \times 25 \text{ km}^2$) twenty year (2000–2019) monsoon-rainfall (June to September averaged) derived from IMD measurements (Indian Meteorological Department) and identify the regional spatial modulations in monsoon-rainfall over



India mainland. Further, to get insights delineating the rainfall changes due to aerosol in comparison to the atmosphere without aerosols (i.e. considering only the greenhouse gas (GHG) warming effect) over the Indian subcontinent, we evaluate the aerosol-monsoon interactions from long-term historical simulations (1901 to 2014) in a global aerosol climate model. Furthermore, to understand the regional aerosol-monsoon interactions examining the regional spatial modulations in the measured rainfall, ARS is setup adequately accounting for regional aerosol distributions and their radiative effects in a fine-resolved regional aerosol climate model. The ARS is designed to evaluate the aerosol species-wide (dust and anthropogenic) impact, potential underlying mechanism governing aerosol-induced rainfall spatial modulations and assessing sensitivity of anthropogenic aerosols control to gain water management benefits.

2.1 Aerosol Response Simulation (ARS): aerosol scenarios, mechanism, and control

We conduct the fine grid resolved ($25 \times 25 \text{ km}^2$) aerosol response simulation (ARS) over the Indian region (including the region between 7.1°N to 34.1°N and 68.6°E to 96.4°E) in a recently developed augmentation of the advanced research version of the weather research and forecasting model (WRF), WRF-Solar.

2.1.1 Designing aerosol scenarios for ARS

The aerosol species-wide (anthropogenic, dust) optical properties (AOD, SSA, and AE) for the monsoon season are estimated with OPTical properties SIMulation (Stromatas et al., 2012) (OPTSIM) using the atmospheric layer-wide concentration of aerosol species from the constrained aerosol simulation approach (*constrsimu*) developed in our previous study (Kumar et al., 2018). The *constrsimu* was designed in a previous study (Kumar et al., 2018) with the aim of delivering a better resemblance between model estimates and observations of atmospheric aerosol species and predicting their spatial distribution as consistently as possible. This approach is based on constraining the simulated AOD in a free-running aerosol transport simulation performed with the general circulation model (GCM) of Laboratoire de Météorologie Dynamique (LMDZT-GCM) (Hourdin and Armengaud, 1999) with the observed AOD to surpass the discrepancy induced specifically by emissions in the source region. Species-wide constrained AOD is then used in an inversion algorithm to estimate the aerosol species-wide concentration at 19 vertical layers of the model (having five layers below 600 hPa and nine layers above 250 hPa). A good agreement was seen between the *constrsimu* estimated aerosol species concentration and the respective observations. In this regard, aerosol species surface concentrations of black carbon (BC), organic carbon (OC), and sulfate-other water-soluble (Sul-ows) estimated from *constrsimu* amounted to 70%–100% compared to free running LMDZT-GCM being 20%–50% of their measured counterparts (Kumar et al., 2018).

In the present study, the aerosol species-wide concentrations (19-vertical layers) so estimated (as mentioned above) for the monsoon season (June to September) are used in OPTSIM to develop aerosol optical properties for aerosol scenarios. OPTSIM (Stromatas et al., 2012) is a numerical model to calculate the tropospheric optical properties from aerosol concentration fields from the chemistry transport model (CTM). The aerosol optical properties for the following aerosol scenarios were developed from OPTSIM simulations,



1. anthropogenic aerosol, using concentrations and properties each of BC, organic carbon (OC), Sul-ows, and inorganic matter (IOM) only,
- 125 2. dust aerosol, using concentrations and properties of dust only,
3. all-aerosol, using concentrations and properties each of BC, OC, Sul-ows, IOM, dust, and sea salt (SS) together.
4. no-aerosol, i.e. atmosphere without aerosols and with GHG only.

2.1.2 Fine-grid resolved ARS in regional climate model (WRF-Solar)

The WRF-Solar is specifically developed for the enhanced prediction of solar irradiance (Haupt et al., 2016; Jimenez et al.,
130 2016). It utilizes an improved numerical weather prediction (NWP) model for calculating solar power and impact. The Rapid Radiative Transfer Model for GCMs (RRTMG) scheme (Iacono et al., 2008) has been used for shortwave parameterization. The parameterization had been found to be producing an accurate estimation of surface irradiance given accurate aerosol optical properties (Ruiz-Arias et al., 2013). A simplified representation of the Thompson micro-physics for the aerosol interaction (Thompson and Eidhammer, 2014) is used to enable cloud-aerosol feedback and maintain computational affordability. The
135 combination of the RRTMG radiation scheme and the (Thompson and Eidhammer, 2014) micro-physics scheme fully incorporates the first and second aerosol indirect effects (Twomey et al., 1974; Albrecht, 1989). In earlier studies, the cloud particle size for shortwave radiation calculations was imposed (i.e., the cloud effective radius is forced to remain constant) internal to a particular radiation scheme; however, consistent cloud particle distributions in the micro-physics and radiation scheme are used in the present simulations. To achieve a more consistent physical representation of the cloud-radiation feedback and activate
140 the aerosol indirect effects, we passed the effective radius of the cloud droplets, ice, and snow particles from the micro-physics to the radiation (both shortwave and long-wave) parameterization. The extinction coefficient is passed to the aerosol parameterization for radiation at each time step. A mass-flux-based shallow convection scheme (Deng et al., 2003, 2014) is used, which includes a cloud entraining/detraining model to represent updrafts triggered by factors including planetary boundary layer depth and turbulent kinetic energy (TKE). We used a hybrid closure combining TKE and convective available potential
145 energy, depending on the updraft depth.

ARS for each of the four aerosol scenarios is conducted corresponding to five different climatic conditions (two La-Niña years each with positive or negative IOD, two El-Niño years each with positive or negative IOD, and one neutral year) prevalent during monsoon periods (refer to Table S1 in Supplementary Information). The ARS is conducted for the aerosol scenarios but with the same amount of aerosol burden under different climatic patterns. The above combination of five climatic conditions and
150 four scenarios (all-, anthropogenic, dust, and no-aerosols) lead to conducting twenty numbers of aerosol response simulations. The aerosol-induced perturbations or changes are estimated by calculating the relative change in radiative effect and rainfall for aerosol scenarios with respect to the no-aerosol scenario. The estimates from ARS under the different climatic patterns are also used to estimate the probability density (PD) of rainfall change for the aerosol scenarios over the selected regions ‘R1’ and ‘R2’.



Besides, to examine the potential underlying mechanism of aerosol-induced change in rainfall, the aerosol-induced perturbations or changes are also estimated for wind field dynamics and hydro-meteorological parameters by calculating their relative change due to aerosol scenarios with respect to the no-aerosol scenario.

2.2 Radiative perturbations due to aerosol types

The downward and upward shortwave radiative flux ($SWRF_{down}$ & $SWRF_{up}$ respectively) are simulated at the top of the atmosphere (TOA) and surface (SUR) for each of the above-mentioned four scenarios (i.e., *all – aerosol*, *anthropogenic – aerosol*, *dust – aerosol*, and *no – aerosol*). We present in the manuscript the all-sky (with clouds; direct+indirect) and clear-sky (without clouds; direct) aerosol radiative effects (ARE) at SUR. The change in the shortwave radiative flux ($SWRF_{down} - SWRF_{up}$, δ_{SWRF}) at the SUR is estimated for respective aerosol scenarios (i.e. $\delta_{SWRF, all}^{SUR}$, $\delta_{SWRF, anthro}^{SUR}$, $\delta_{SWRF, dust}^{SUR}$) (equation 1-3). The ARE due to aerosol scenarios ($ARE_{all-aerosol}$, $ARE_{anthropogenic-aerosol}$, $ARE_{dust-aerosol}$) at SUR is calculated by taking the difference between corresponding δ_{SWRF} and $\delta_{SWRF, null}$ (equation 1-3). It is to be noted that the aerosol-induced change for rainfall, wind field distribution, and hydro-meteorological parameters as obtained from ARS in WRF and shown in the manuscript is due to aerosol all-sky radiative effects. We have also shown the changes in rainfall and wind fields due to aerosol clear-sky radiative effects in the Supplementary Information. The above including four aerosol scenarios under five climatic patterns, thereby twenty numbers of ARS for clear-sky, besides the same for all-sky, thus a total of forty numbers of ARS, are used in the analysis.

$$ARE_{all}^{SUR} = \delta_{SWRF, all}^{SUR} - \delta_{SWRF, null}^{SUR} = (SWRF_{down, all}^{SUR} - SWRF_{up, all}^{SUR}) - (SWRF_{down, null}^{SUR} - SWRF_{up, null}^{SUR}) \quad (1)$$

$$ARE_{anthro}^{SUR} = \delta_{SWRF, anthro}^{SUR} - \delta_{SWRF, null}^{SUR} = (SWRF_{down, anthro}^{SUR} - SWRF_{up, anthro}^{SUR}) - (SWRF_{down, null}^{SUR} - SWRF_{up, null}^{SUR}) \quad (2)$$

$$ARE_{dust}^{SUR} = \delta_{SWRF, dust}^{SUR} - \delta_{SWRF, null}^{SUR} = (SWRF_{down, dust}^{SUR} - SWRF_{up, dust}^{SUR}) - (SWRF_{down, null}^{SUR} - SWRF_{up, null}^{SUR}) \quad (3)$$

2.3 Long-term historical global aerosol-climate simulations: IPSLCM6A-LR (CMIP6 experiments)

As mentioned earlier, we utilise the simulated precipitation (pr) data, in $\text{kg m}^{-2} \text{s}^{-1}$ (horizontal resolution of $2.5^\circ \times 2.5^\circ$) from IPSL-CM6A-LR: Version 6 (Boucher et al., 2020) for Climate Model Intercomparison Project Phase 6 (CMIP6) experiments of long term simulations (1850 to 2014). The historical global aerosol-climate simulations are analysed for the present years (1995–2014) considering the atmosphere (i) with no-aerosols, referred to as hist (no-aerosol) scenario; and (ii) with aerosols (i.e. aerosols and GHG), referred to as hist (aerosol) scenario. The relative (%) change in rainfall in present years relative to the pre-industrial climatology (1901 to 1930) for the above-mentioned two scenarios and that due to aerosols is examined identifying the spatial concordance in rainfall modulations between model and measurements.



3 Results

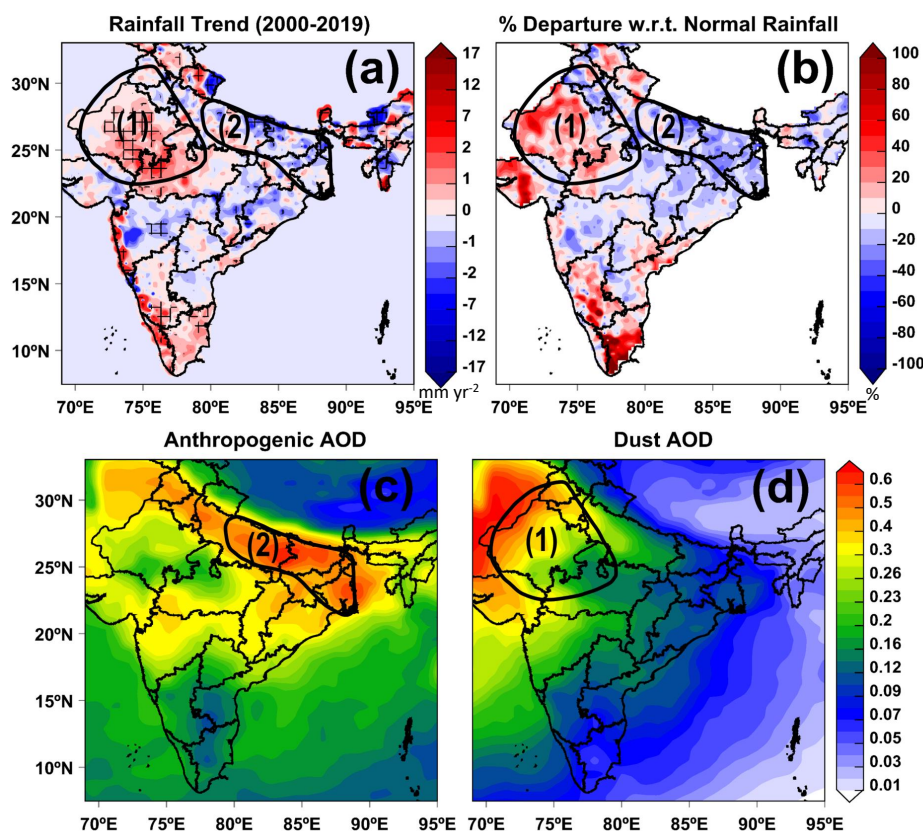


Figure 1. (a) Spatial distribution of the temporal trend (over the period of 2000 to 2019) of Indian summer monsoon (monsoon) rainfall from measurements of Indian Meteorological Department (IMD-rainfall) (mm yr^{-2}); The black '+' symbols over shaded regions represent significance at 90% confidence level). (b) Average percentage (%) departure or divergence over the selected years of the IMD-rainfall from the defined normal monsoon of the respective year. Spatial distribution of monsoon AOD due to (c) Anthropogenic aerosols, and (d) dust aerosols.

3.1 Spatial concordance: monsoon rainfall, aerosol optical depth (AOD) due to anthropogenic and dust aerosols

To identify the spatial modulations of monsoon-rainfall over the Indian subcontinent, we analyse the spatial distribution (25×25 km²) of monsoon-rainfall from the Indian Meteorological Department measurements (IMD-rainfall: June to September) presenting the temporal trend over a twenty-year (2000–2019) period (Figure 1a) and the percentage departure (Figure 1b). The percentage departure of the IMD-rainfall is obtained as the divergence of the IMD-rainfall of a selected year from the defined normal monsoon of the respective year averaged over the five selected years. The five selected years are taken accounting for the changing meteorological climatic patterns during monsoon corresponding to five different climatic conditions (two La-Niña years each with positive or negative Indian-ocean dipole (IOD), two El-Niño years each with positive or negative



IOD, and one neutral year) (also refer to section ‘Aerosols induced spatial changes in monsoon-rainfall from aerosol response simulations (ARS): concordance with measurements’ and Table S1 in Supplementary Information). The negative departure or divergence indicates the reduction or deficiency in actual monsoon-rainfall compared to the normal and vice versa for the positive departure or divergence. The normal monsoon for a respective year is estimated as the mean of the last 50 years of
200 IMD-rainfall (Indian Meteorological Department). Patches of spatially changing patterns of monsoon-rainfall (decreasing or increasing temporal trends and positive or negative departures of the actual monsoon-rainfall from the normal) are visualised over mainland India. While a decreasing trend ($1-7 \text{ mm yr}^{-2}$) in recent years is seen over most of the Indian region, including the areas of the IGP, eastern coast, and western India (areas of Maharashtra region); patches of increasing trend ($1-6 \text{ mm yr}^{-2}$) is visualised over the areas of northwestern India, central India, western coastline and southern India. The locations or points
205 of an increasing or decreasing monsoon-rainfall trend which is statistically significant at 70% confidence level are also marked in Figure 1a. It is observed that regions or locations witnessing the negative and positive departure (20% to 50% in most areas) from the normal monsoon-rainfall (Figure 1b) are in general spatially overlapping with that comprising of the decreasing and increasing trend, respectively.

To examine the spatial changes in the aerosol burden by species type (anthropogenic or dust) over the Indian subconti-
210 nent, we further present the AOD due to anthropogenic (AOD-anthro, Figure 1c) and dust (AOD-dust, Figure 1d) aerosols averaged during the monsoon (June to September). The AOD-anthro and AOD-dust are estimated in OPTical properties SIMulation (OPTSIM), a numerical model to calculate tropospheric optical properties from the derived aerosol concentrations (refer to “Methods”). The aerosol species distribution over India is obtained from the constrained aerosol simulation approach which was found to satisfactorily represent the observed values (Kumar et al., 2018). The AOD-anthro is the sum of AOD
215 due to sulphate and other water-solubles ($\text{AOD}_{\text{Sul-ows}}$), black carbon (AOD_{BC}), organic carbon (AOD_{OC}), inorganic matter (AOD_{IOM}) (refer to Figure S2 in the Supplementary Information). While the large value of AOD-dust (> 0.3) is prominent mostly over the northern IGP and northwestern India (Figure 1d), the AOD-anthro (> 0.3) is that over the IGP, eastern coast, and the western India (Figure 1c). While the largest atmospheric burden of anthropogenic aerosols over the IGP is mainly attributed to a large population density, varying anthropogenic activities, including influence due to meteorology and geo-
220 graphical location of the IGP (Ghosh et al., 2021; Verma et al., 2022; Ghosh and Verma, 2023). This of desert dust over the northern IGP and northwestern India is due to transport from desert locations in nearby (western India, Thar desert) and far-off regions (e.g. west Asia) (Verma et al., 2008; Kumar et al., 2018; Kumar and Verma, 2016). Interestingly, the spatially varying AOD-dust and AOD-anthro are in general visualized to be spatially concordant to the observed spatial modulations comprising of strengthening and weakening IMD-rainfall (from trends and departures, Figure 1a-b), respectively. Nevertheless, the
225 enhanced IMD-rainfall (from trends and departures) is also seen over areas of central and southern India, and the western coastline with a relatively lower anthropogenic or dust aerosol burden. The spatial heterogeneity in aerosol species (anthropogenic and dust) distribution may exert a non-uniform aerosol radiation perturbations across the Indian subcontinent, which have implications for aerosol-driven monsoon-rainfall spatial modulations, as discussed in the subsequent sections.

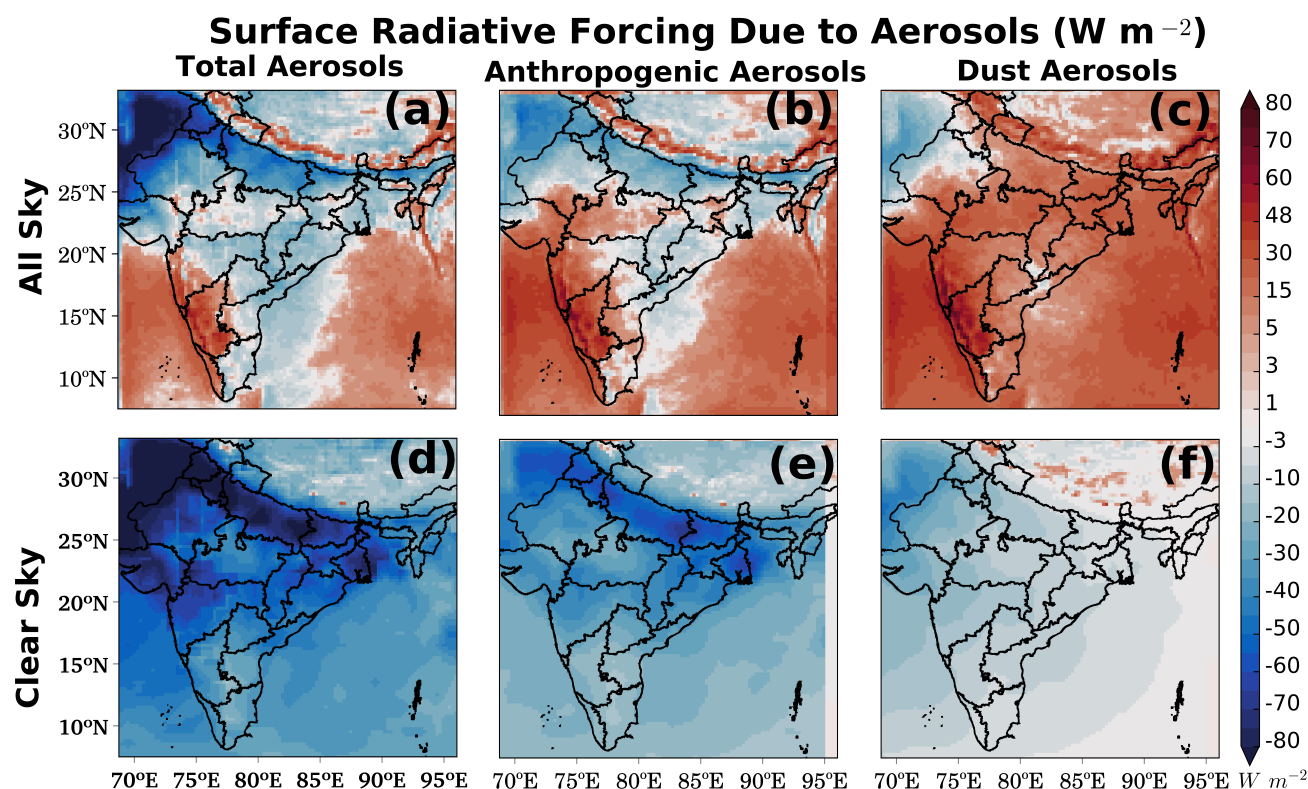


Figure 2. Aerosol radiative forcing averaged during monsoon period at surface (SUR) for all sky (upper panel, a–c) and clear sky (lower panel, d–f) due to all aerosols (a,d), anthropogenic aerosols (b,e), and dust aerosols (e,f)

3.2 Radiative perturbation due to aerosol species over the Indian subcontinent: impact of anthropogenic and dust aerosols

230

The spatial distribution of all-sky surface radiative effects during the monsoon is shown in Figures 2a–c. The aerosol radiative effects (Figures 2a–c) are estimated due to all-aerosols and that segregated by aerosol species type, i.e. anthropogenic- and dust aerosol. These estimates correspond to the designed aerosol scenarios in ARS, i.e. considering the atmosphere with anthropogenic aerosol species (see AOD-anthro), dust (see AOD-dust), all-aerosols (anthropogenic+dust+sea salt) relative to no-aerosols (refer to section 2).

235

The all-sky surface radiative effects due to all-aerosols are found to exhibit radiative cooling (negative values of radiative effect) over most of the Indian subcontinent (larger than $-40 W m^{-2}$ over most of the IGP) including the coastal Bay of Bengal (BoB), but, radiative warming (15 to $30 W m^{-2}$) over the western coast, northwestern India, areas of central India, and the oceanic regions of the Arabian Sea (AS) and the farther BoB (away from coastal). The all-sky aerosol radiative warming over the AS found in the present study is in corroboration with a previous study inferring rapid surface warming in the northern AS

240



and adjacent northwestern India to explain the extreme rainfall events in the central India region (Roxy et al., 2017). However, our study also explains the underlying mechanism due to all-sky aerosol-driven radiative warming (see section “Potential mechanism for the monsoon-rainfall pattern: aerosols induced impact on regional-scale hydro-meteorological parameters”) which is not explained in the previous study. The spatial variation of all-sky surface radiative forcing due to anthropogenic aerosols is similar to all-aerosol scenario but with a relatively larger spatial extent of radiative warming (specifically over regions with low anthropogenic aerosol burden). In contrast to the above, the all-sky surface radiative forcing due to dust exhibits mainly radiative warming over most of the Indian subcontinent.

In comparison to spatially varying all-sky aerosol surface radiative warming or cooling, the clear-sky aerosol surface radiative effects exhibit radiative cooling across the Indian subcontinent and for all the three aerosol scenarios (Figures 2d-f). The magnitude of clear-sky radiative cooling depending upon the relative distribution of species-wide AOD is the largest due to all-aerosols, followed by anthropogenic and dust. The above in turn has an impact on the aerosol species-wide changes in the all-sky aerosol radiative warming or cooling effects. The clear-sky surface radiative cooling due to dust aerosols is lower than the anthropogenic- and all-aerosols; thereby influencing a larger all-sky radiative warming due to dust. Similarly, the clear-sky surface radiative cooling due to anthropogenic- or all-aerosols compensates for the all-sky radiative warming due to the respective aerosol scenarios. In general, the clear-sky aerosol surface radiative cooling of lower than 30 W m^{-2} (along eastern coast and BoB) to 50 W m^{-2} (along the western coast and AS) is found to exert an all-sky aerosol radiative warming in the vicinity of relative distribution of cloud fraction. A large cloud fraction due to aerosols (higher by more than 50% relative to no-aerosol) is indeed estimated along the western coast, AS, northwestern India, and areas of central-western India (refer to Figure 4f discussed later).

3.3 Aerosols-driven monsoon-rainfall spatial modulations from global aerosol climate model: concordance with measurements

To get insights on the aerosol-driven monsoon-rainfall modulations over the Indian subcontinent, we first evaluate the available long-term simulations (1901 to 2014) of monsoon-rainfall, from global aerosol climate model (IPSLCM6A-LR, horizontal resolution: $2.5^\circ \times 2.5^\circ$) in CMIP6 experiments (O'Neill et al., 2016). These simulations are analysed for the present years (1995–2014) considering the atmosphere (i) with no-aerosols (i.e. atmosphere with greenhouse gases (GHG)-only), referred to as hist (no-aerosol) scenario; and (ii) with aerosols (i.e. aerosols+GHG), referred to as hist (with-aerosol) scenario. The relative (%) change in rainfall in present years relative to the pre-industrial climatology (1901 to 1930) for the above-mentioned two scenarios is presented in Figures 3a and 3b, respectively. The change in rainfall for hist (no-aerosol) scenario does not represent or is opposed to the observed pattern of spatial modulations in the measured monsoon-rainfall (Figure 1a-b). It exhibits a relatively increasing pattern (by 20% to 50% of the rainfall during pre-industrial climatology) over the entire Indian region and a decreasing to neutral along the western coast and central India. In contrast to hist (no-aerosol) scenario, the spatial modulations in rainfall for hist (with-aerosol) scenario (Figure 3b) show-up similar spatial features to the measured monsoon-rainfall, including a relatively decreasing pattern of rainfall over areas of the IGP, but with a slightly increasing rainfall along the southern coast (e.g. around Kerala region). The above discussion thus reveals the regional spatial modulations (from measured



trends and departures) in IMD-rainfall comprising of rainfall-deficient and rainfall-excessive areas as identified over the IGP and western India, respectively, are aerosol-driven and can not be explained by GHG warming.

To delineate the change in rainfall due to aerosols during present years relative to the pre-industrial climatology (Figure 3c), we take the difference of (i) from (ii) above. The relative decrease in rainfall (10% to 30% of the rainfall during pre-industrial climatology) attributable to aerosols is visualised over most of the areas of mainland India with the largest deficiency (20% to 30%) seen over the northern IGP. Interestingly, the increased rainfall (10% to 30%) along the western coast and the southern coast (along Kerala region), and the central-western areas is also found to be appearing due to aerosols, unlike the contrasting patterns for (i) above (Figure 3a). Thereby indicating the regional spatial modulations observed in IMD-rainfall (trend and departures) are in general well represented by the spatial changes (weakening and strengthening) in rainfall imposed due to aerosol during present years. The estimated rainfall deficiency and enhancement relative (%) to pre-industrial rainfall are lower in magnitude than the measured departures (%) in IMD-rainfall. The above is expected from global aerosol simulations due to a coarser resolution and an inadequate regional aerosol burden (Ghosh et al., 2021) in the global climate model, and thereby lack of model capability to adequately resolve the aerosol-driven spatial modulations in monsoon-rainfall.

3.4 Aerosols-driven monsoon-rainfall spatial modulations from ARS in regional climate model: concordance with measurements, impact of anthropogenic and dust aerosols

To assess the aerosol-induced spatial modulations in rainfall at a fine-grid scale over the Indian subcontinent evaluating the role of dust and anthropogenic aerosols, we examine the estimates from the designed ARS in a fine-grid resolved aerosol climate model. To represent the aerosol-driven modulations on monsoon-rainfall as realistically as possible, accounting for the aerosol-meteorological interactions, the change in modelled monsoon-rainfall due to aerosols is estimated finding out the difference between modelled rainfall considering the atmosphere with aerosols and that without aerosols or no-aerosols. We compare the measured departures from IMD-rainfall with the modelled aerosol-induced change in rainfall from the designed ARS averaged over the selected years. The measured departures are used as we believe the above estimates from measurements would consistently represent the regional spatial modulations (rainfall deficiency or excessiveness) induced due to aerosols irrespective of the rainfall changes from global climatic patterns across the entire Indian subcontinent, thus aiding to compare the modelled and measured values of aerosol induced rainfall change and identify the regional hotspots for mitigations.

The spatial distribution of the modelled percentage change in the rainfall due to all-aerosols scenario (relative to no-aerosol) averaged over the five selected years corresponding to five different climatic conditions is shown in Figure 3d. The decreasing rainfall (mostly by 40% to 50%) is visualised over most of the Indian subcontinent, including the IGP region and oceanic region of the Bay of Bengal (BoB). Patches of spatially increasing rainfall (mostly by 30% to 60%) are also visualized over northwestern India (areas of Rajasthan and Gujarat), south-eastern coast (including Andhra Pradesh), with a specifically large value along the western coast (including coastal areas of Maharashtra, Karnataka, and Kerala). Notably, contrasting features of aerosol-induced spatial modulations are visualised over the adjoining oceanic regions of the BoB and AS, comprising of rainfall deficiency over the BoB and a neutral to slight strengthening over the AS. The modelled spatial modulations (increasing or decreasing) in the simulated rainfall due to the all-aerosol across the above-mentioned regions over mainland India are in

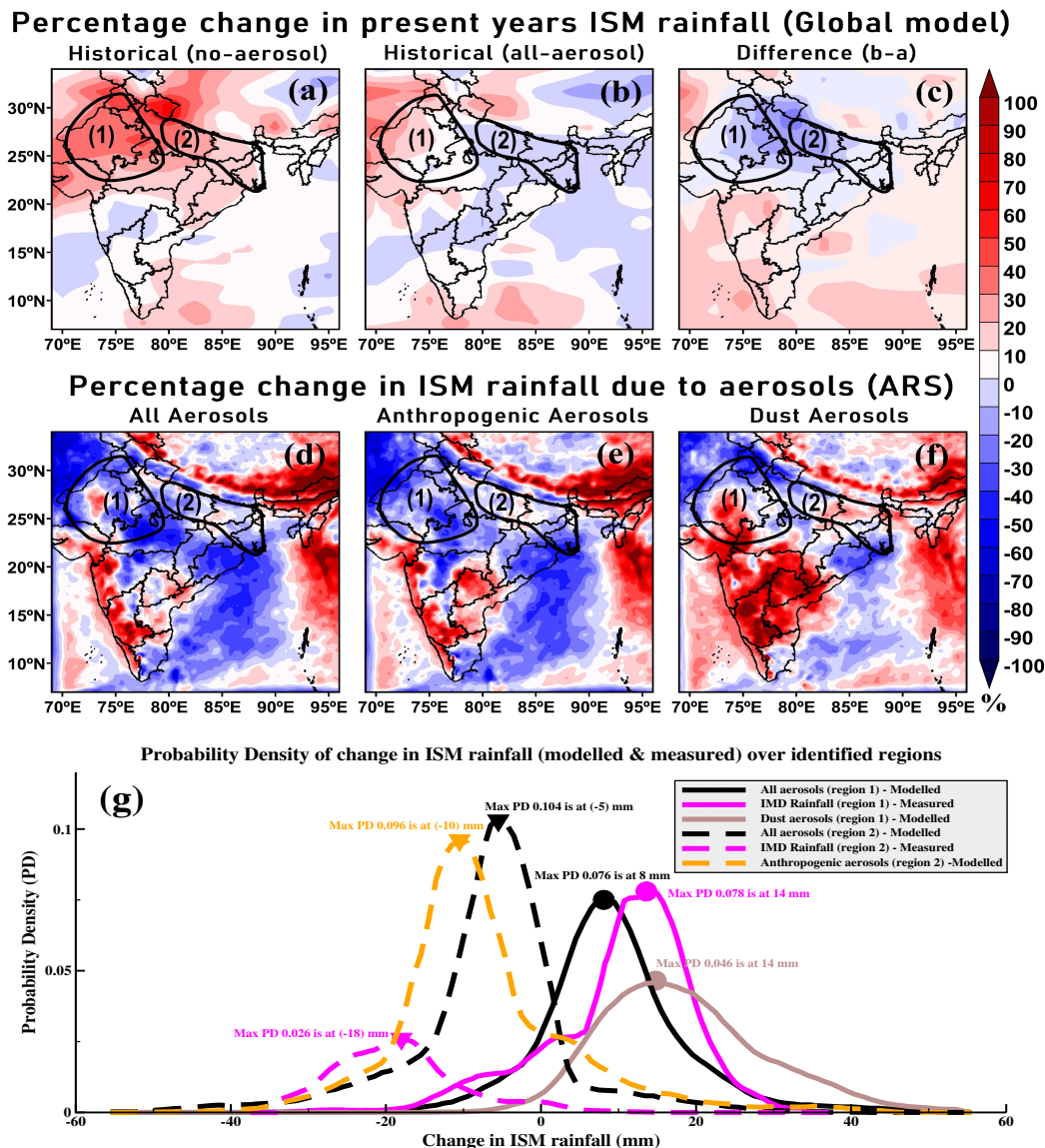


Figure 3. (a-c) Spatial distribution of change in monsoon-rainfall from simulations in global aerosol climate model estimated for present years (relative to pre-industrial) considering atmosphere (a) without-aerosols (with ghg forcing only), (b) with-aerosols (ghg and aerosols), (c) due to aerosols (difference between (a) and (b)); (d-f) Spatial distribution of change in monsoon-rainfall from ARS in regional aerosol climate model averaged over selected years (relative to no-aerosol), ($\frac{\text{with aerosols} - \text{no aerosols}}{\text{no aerosols}} \times 100$), due to (d) all aerosols, (e) anthropogenic aerosols, and (f) dust aerosols; (g) Probability density (PD) of rainfall change as modelled due to all-aerosols, anthropogenic and dust aerosols for the identified regions (rainfall-excessive, 'R1': 974 gridpoints and rainfall-deficient, 'R2': 477 gridpoints) averaged over 5-y corresponding to the five types of climatic patterns during the monsoon period. The same as above but that obtained from IMD-rainfall departures is also shown. The magnitude of rainfall change corresponding to the maximum probability density is also marked.



spatial concordance with the corresponding modulations observed from measurements, i.e. IMD-rainfall (trends and departures,
310 Figure 1a-b).

We find that all-aerosol-induced spatially decreasing and increasing rainfall is primarily governed by the presence of anthropogenic and dust aerosols, respectively (Figure 3e-f). An exception to the above, few patches of all-aerosol-induced increasing rainfall features as visualized over locations along the western coast, and parts of the eastern coast do concur as the same feature from both anthropogenic and dust aerosols (Figure 3e-f). However, the increasing feature of rainfall is enhanced with
315 a larger spatial advancement from dust compared to anthropogenic over these locations, specifically covering more of central and western and northwestern India. The spatial advancement over central India of aerosol-induced increasing monsoon from dust aerosols as obtained from ARS is also supported by the observational studies inferring an increasing trend in heavy to extremely heavy rainfall events in the central Indian region in recent decades (Roxy et al., 2017). Further, aerosol-induced increasing monsoon from both dust (Figure 3f) and anthropogenic (Figure 3e) aerosols as obtained from ARS is also in cor-
320 roboratorion with the increased rainfall events witnessed during the monsoon seasons in recent years (2018 and 2019) at the southern tip of India (Kerala) and over the southern parts of the west coast of India (Vijaykumar et al., 2021). Though the spatial locations identified in the present study with aerosols-induced increased rainfall corroborate with the regions reported with heavy rainfall or extreme flood events in available studies. The heavy rain statistics induced due to aerosols including the ocean memory effect from large-scale climate patterns and their temporal concurrence with the available studies need to
325 be further assessed in a future study. The increased rainfall due to aerosols over areas of relatively low anthropogenic burden (e.g. western coast comprising areas of Karnataka and Kerala regions) as shown in the present study is also supported by a recent study (Kripalani et al., 2022) inferring increased rainfall over south and southeast Asia during COVID 2020, based on evaluating measured rainfall (relatively coarsely resolved ($2.5^\circ \times 2.5^\circ$), Global Precipitation Climatology Project and National Center for Environmental Prediction), when the atmospheric pollutants burden was found to be reduced (Dumka et al., 2021)
330 as compared to other years.

To carry out a detailed statistical analysis for the rainfall deficiency and strengthening due to aerosols, we also identify specifically the two regions (see Figure 1) exhibiting distinct distribution of predominating aerosol species type and spatial modulations from IMD-rainfall as follows: (i) area over northwestern India (Region 1, 'R1', or rainfall-excessive region): comprising of AOD being predominantly due to AOD-dust, and including the observed strengthening IMD-rainfall (trends and
335 departures); (ii) area over the IGP (Region 2, 'R2', or rainfall-deficient region): comprising of AOD being predominantly due to AOD-anthro, and including the observed weakening IMD-rainfall. Over the identified regions of 'R1' (northwestern India, where dust burden is predominant) and 'R2' (IGP region where anthropogenic aerosols are predominant), about 60% to 80% of grids comprise, respectively, increasing and decreasing rainfall values due to dust (Figure 3f) and anthropogenic aerosols (Figure 3e). While the maximum rainfall deficiency for the region 'R2' in the presence of anthropogenic aerosols is estimated
340 over eastern coast gridpoints (average across gridpoints with rainfall deficiency: 58%), the maximum rainfall increase for region 'R1' in the presence of dust aerosols is estimated over northwestern India gridpoints (average across gridpoints with rainfall strengthening: 70%).



The Probability density (PD) of modelled rainfall change for all-aerosols, anthropogenic and dust aerosols over the identified regions (rainfall-excessive, 'R1': 974 gridpoints and rainfall-deficient, 'R2': 477 gridpoints) averaged over 5-y corresponding to the five types of climatic patterns during the monsoon period is shown in Figure 3g. We also present the PD of measured rainfall change (Figure 3g) obtained from IMD-rainfall departures averaged over the same period as mentioned above. Most of the area ($> 70\%$) of the PD distribution curve of the rainfall change due to all-aerosols and dust aerosols over region 'R1' comprise the increasing rainfall (or positive) values relative to no-aerosol. The peak of the PD curve corresponding to the maximum frequency of magnitude of rainfall increase lies at +8 mm for all-aerosols compared to being +14 mm for dust aerosols. In contrast to that for 'R1', a large area of the PD distribution curve of the rainfall change due to all-aerosols and anthropogenic aerosols over region 'R2' comprises of the decreasing rainfall (or negative) values relative to no-aerosol. The peak of the PD curve lies at -5 mm for all-aerosols compared to that being -10 mm for anthropogenic aerosols. Consistent with the modelled values, most of the area of the PD distribution curve of the rainfall change from IMD-rainfall comprises of the decreasing rainfall (or negative) values for 'R2' and vice versa for 'R1'. Also, the maximum PD of the rainfall change from IMD-rainfall at +14 mm (-18 mm) for 'R1' ('R2') is found to be closely matching with the modelled values of rainfall change due to dust (anthropogenic aerosols) for 'R1' ('R2').

More details on the statistical analysis of modelled aerosol-induced rainfall deficiency and strengthening averaged over the five selected years corresponding to five different climatic conditions and its comparison with the corresponding changes from IMD-rainfall departures for the identified 'R1' and 'R2' regions are further discussed in the Supplementary Information (refer to section 'Comparison of modelled aerosol induced rainfall change with IMD-rainfall: statistical analysis'; and Table S2). Our comparison presented in the study thereby indicates modelled aerosol-induced (anthropogenic and dust) spatial modulations (weakening and strengthening) of monsoon-rainfall and their respective magnitudes over the Indian subcontinent corroborates the measured spatial modulations (departures) in IMD-rainfall. A reasonably good comparison of measured departures with the modelled aerosol-induced spatial modulations indicates that the measured spatial modulations (weakening and strengthening as departures) in the monsoon-rainfall are driven by regional aerosols over the Indian subcontinent. Thereby confirming our hypothesis on the modelled aerosol-induced changes (relative to no-aerosol) using the designed ARS to consistently represent the measured spatial modulations in the monsoon-rainfall.

3.5 Potential mechanism of aerosol-driven monsoon-rainfall spatial modulations: evaluating wind-fields

To evaluate the mechanism of the aerosol-induced change in the monsoon, we examine the regional dynamical response visualizing the aerosol-induced relative change (compared to no aerosol) in the regional wind fields (wind direction and wind speed) distribution. The spatial distribution of the enhancing dynamical impact (+ve values) indicates the aerosols-induced positive forcing (increased intensity and the same direction) of the large-scale monsoon flow from no-aerosol scenario simulation (Figure 4a) and is vice versa for the suppressing dynamical impact. The color scale (Figures 4b-d) represents the enhancing (+ve values: red color on color scale) and suppressing (-ve values: blue color on color scale) dynamical impact of aerosols (Figures 4b-d) on the climatological wind-fields pattern (no aerosols scenario, Figure 4a).

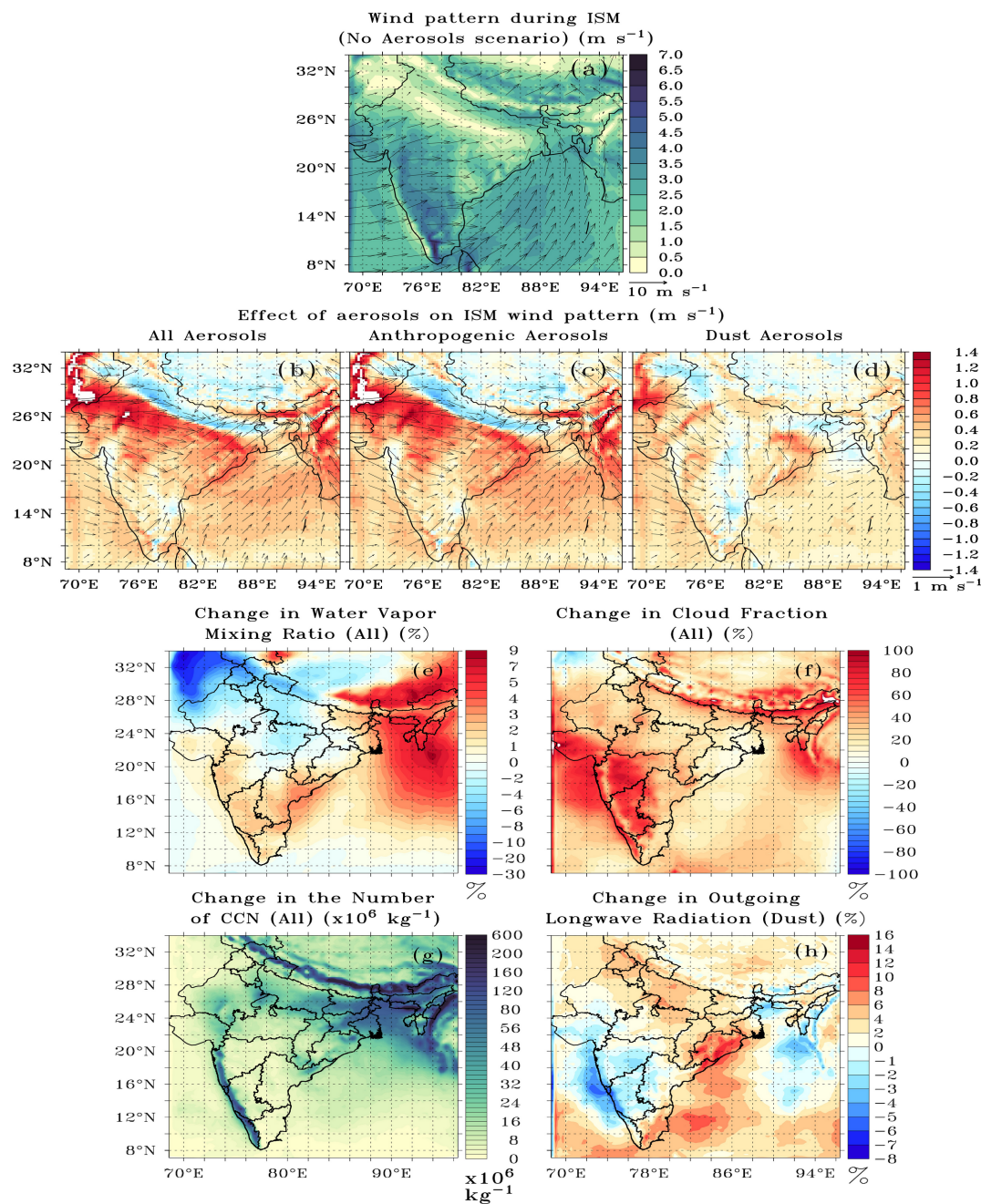


Figure 4. (a-d) Simulated wind-fields for (a) no-aerosols (atmosphere without aerosols) scenario; Change in wind-fields (w.r.t no-aerosols scenario) due to (b) all-aerosols, (c) anthropogenic aerosols, and (d) dust aerosols. The color scale represents the enhancing (+ve values: red color on color scales) and suppressing (-ve values: blue color on color scale) dynamical impact of aerosols on the climatological windflow pattern (no aerosols scenario); (e-f) spatial distribution of simulated percentage change (%), w.r.t no-aerosols) due to all-aerosols scenario in the (e) water vapor mixing ratio (%), and (f) cloud fraction (%); simulated change (w.r.t no-aerosols) in the (g) number of cloud condensation nuclei (CCN) ($\times 10^6$) for all-aerosols scenario; (h) outgoing long-wave radiation (OLR) (W m^{-2}) for dust aerosols.



The monsoon wind-fields circulation (no-aerosol scenario, Figure 4a) over the Indian Ocean indicates an intrusion of climatological south-western monsoonal flow (3 to 4 m s^{-1}) inside the Indian mainland from the Arabian Sea along the western coast and from the Bay of Bengal along the eastern coast at lower eastern IGP. It is also seen that change in the wind pattern from all-aerosols has an enhancing impact (by 0.2 to 0.8 m s^{-1}) on the climatological south-westerly wind (no-aerosol) over the oceanic region of the BoB. The aerosol-induced anomalous change forces a diversion of the wind vectors away from the Indian mainland along the lower eastern IGP compared to the climatological monsoonal south-westerly flow (no-aerosol) intruding the Indian mainland from the Bay of Bengal. We see the presence of both the enhancing and suppressing dynamic impact on the climatological wind pattern over the IGP. While the suppressing impact (blue-colour pattern) to the climatological easterlies (no-aerosol, Figure 4a), thus, resulting in a westerlies wind pattern (0.2 to 0.6 m s^{-1}) is visualized over the IGP region adjacent to Himalayan foot-hills. The enhancing impact (red-colour pattern) to a low-intensity climatological south-westerly wind pattern, thus, resulting in an increased north-westerly wind (1 to 1.4 m s^{-1}) as visualized over the IGP and central India. The changed wind-field dynamics over the IGP region displaying a suppressing impact indicates a decrease in moisture-bearing air masses rather than from the Bay of Bengal region in the climatological (no-aerosol) scenario. However, the increased intensity of the north-westerly wind over the IGP region displaying an enhanced impact strengthens an increased potential of desert dust influx from northwestern India and west Asia to the IGP and central India.

Both the aerosol-induced enhancing and suppressing dynamical impact on the climatological wind pattern over the IGP thus, enforce the wind flow from land towards the ocean rather than from the oceanic region over the IGP. It is to be noted that the aerosol-induced change presented in Figure 2 is due to all-sky aerosol radiative effects in WRF. It is found that including only the clear-sky aerosols radiative effect in ARS showed a similar pattern of spatial change in wind fields, including enhanced or suppressed dynamical impact as with the all-sky radiative effect but with much-decreased values (refer to Figure S3 in the Supplementary Information for all-aerosols scenario).

The aerosol-induced change in wind circulation pattern and intensity (Figure 4b) visualised as an enhancing or suppressing dynamical impact to the climatological wind pattern (no-aerosols) is noted to be larger from anthropogenic aerosols (Figure 4c) compared to dust (Figure 4d). Thereby, relatively a few patches of decreasing rainfall are visualised in the dust aerosol scenario over areas of the IGP (as discussed in the previous section). Our study thus reveals the spatially decreasing rainfall is due to the regionally changed wind-field dynamics (direction and intensity), strengthening of the wind flow from land towards the ocean (contrasting the monsoonal flow) as a result of aerosol-induced perturbations in regional radiative energy balance. The aerosol-induced perturbations including stronger aerosol radiative forcing contrasts (radiative cooling and warming) between the ocean and land region from anthropogenic than the dust and that from all-sky than the clear-sky. Besides the above, aerosol-induced radiative effects along the western coast of India enhance the climatological wind pattern (slightly weaker for clear-sky than all-sky) and thereby the monsoonal flow along the western coast of India, favouring an increased rainfall along the western coast and adjoining central India regions. The aerosol-induced increasing rainfall pattern is more prominent for all-sky than clear-sky (refer to Figure S3 in the Supplementary Information), therefore, indicating the aerosol-induced spatially increasing rainfall effect is primarily enforced by aerosol all-sky radiative effects. To assess further a much-enhanced rainfall seen over the



410 above-mentioned regions due to dust aerosols compared to anthropogenic, we further analyze the aerosols-induced change in the hydro-meteorological parameters and dust-induced change in the outgoing long-wave radiation (OLR) in the next section.

3.6 Potential mechanism of aerosol-driven monsoon-rainfall spatial modulations: evaluating hydro-meteorological parameters

The spatial features of water vapour mixing ratio (Figure 4e) from all-aerosols scenario exhibiting an increased amount over the western coastal, northwestern and central region of India, including a decreased amount over areas of the IGP corroborates the features of aerosol-induced spatial modulations in rainfall. The enhanced cloud fraction (Figure 4f) from the all-aerosols scenario (compared to no-aerosols) but with a relatively larger value over the above-mentioned regions is also seen to spatially overlap with the simulated increase in rainfall from dust, anthropogenic, and all-aerosols. The spatially enhanced cloud fraction over the western coastal, northwestern and western-central region of India, has a role in inducing the increased aerosol all-sky radiative warming (refer to section ‘Radiative perturbation due to aerosol species over the Indian subcontinent: impact of anthropogenic and dust aerosols’ and Figure 2a-c) over the region. We also find the increased amount of CCN (Figure 4g) spatially concurs with the aerosols-induced rainfall deficient areas. The reduction in atmospheric moisture content over the regions due to aerosols-induced change in the dynamical impact in conjunction with an increased amount of CCN over these regions due to predominating anthropogenic aerosols (Figure 1b) is favourable to a large amount of but smaller cloud droplets, and causing the aerosols-induced deficiency in rainfall over the region (Figure 3).

On evaluating the dust-induced impact on the OLR (Figure 4h), the reduced OLR from dust aerosols (3% to 8%) compared to the no-aerosols scenario is visualized over the regions with predominant dust influence (e.g. northwestern India, areas of central India, including the western coast of India). Interestingly, the spatial features of the dust-induced reduced OLR spatially overlap with the simulated increase in rainfall from dust aerosols (Figure 4d). The reduced OLR and increased aerosol all-sky radiative warming are favourable to increased convection and thereby an enhanced aerosol-induced rainfall over the above-mentioned region. The above also explains the presence of patches of increased rainfall (refer to Figure 3e) also from anthropogenic aerosol scenario (due to all-sky radiative warming) over the mentioned regions and that its strengthening (due to combined effect both from the reduced OLR and all-sky radiative warming) from dust aerosols. Our study thus shows that the increased rainfall is favoured by the increased convection due to the aerosol-induced all-sky radiative warming in areas having a relatively lower clear-sky aerosol shortwave radiative cooling (e.g. areas predominated by dust or low amount of anthropogenic aerosols, e.g. the western coast, northwestern India, and central India region), and its strengthening due to the dust-induced reduced OLR over the dust-predominant regions.

The dust-induced increase in precipitation pattern over the Indian subcontinent as presented in this study is in corroboration with a previous study (Vinoj et al., 2014) conjecturing the dust-induced heating of the atmosphere over North Africa/West Asia impacting the increased flow of moisture over India and enhanced monsoon-rainfall over central India in the short term. However, our study also finds the dust-induced spatially heterogeneous radiative perturbations governing the measured monsoon-rainfall spatial modulations over the Indian subcontinent successfully simulating the measured departures (not presented in the previous study). The anthropogenic aerosol-induced decrease in precipitation over the Indian subcontinent as



presented in this study is also in corroboration with a previous study (Bollasina et al., 2011) inferring a decreasing trend
445 (1950-1999) in monsoon-rainfall from ensemble simulations of aerosol forcing (as bulk aerosol) in a coarsely resolved GCM.
The above-mentioned study however could not explicitly present role of aerosol species-wide (anthropogenic and dust) spatial
heterogeneity in monsoon-rainfall spatial modulations. Our study also presents anthropogenic aerosols driven spatial modu-
lations (both decreasing and increasing pattern) in monsoon-rainfall including their potential mechanism adequately account-
ing for aerosol distributions in a fine-resolved regional climate model and successfully simulating the measured departures
450 in monsoon-rainfall. We therefore further assess the implications of anthropogenic aerosols control on the required water-
management measures for reducing atmospheric pollutants-induced water-associated societal risks of rainfall-deficiency or
enhancement, as discussed in the next Section.

3.7 Implications of anthropogenic aerosols control on required water-management

Based on our ARS estimates, we locate areas which would require anthropogenic aerosols control or water-management mea-
455 sures, thereby aiding to mitigate aerosol-induced rainfall change for societal benefits. If the anthropogenic aerosol burden is
not controlled, areas which would need the necessary water management measures (from low to high level) to reduce societal
risks due to aerosol-induced increase in rainfall are shown in Figure 5a. These areas are obtained from Figure 3d corresponding
to grids showing enhanced rainfall due to the all-aerosols scenario. However, if control of anthropogenic pollutants is imposed,
then the specific areas where the water management measures should be intensified are marked in Figure 5b. These specific
460 areas (e.g. over grids of Telangana, Andhra Pradesh, Karnataka, Gujarat regions) including areas over the Arabian Sea would
witness further augmented rainfall increase due to the control of anthropogenic aerosols, including that due to the presence of
dust. The above-mentioned areas are spotted within the identified rainfall-excessive regions of Figure 5a, and corresponds to
extracted grids obtained as the difference (mm) between dust-induced (corresponding to Figure 3f) and all-aerosols-induced
(corresponding to Figure 3d) rainfall increase. We also identify locations (patches with blue color on color-scale, Figure 5b)
465 signifying areas which would witness mitigation of increase over rainfall-excessive regions (Figure 5a) and enhancement of
the deficiency over rainfall-deficient regions (Figure 3d) driven by anthropogenic aerosols (lightly to strongly as marked on
the color scale, Figure 5b). In other words, these areas would witness mitigation of rainfall increase driven by control of
anthropogenic aerosols, i.e. along the western coastline (e.g. around coastal Karnataka, Maharashtra (lightly driven); Ker-
ala (moderately driven) and northeastern India (strongly driven). Thereby also identified as target areas within the identified
470 rainfall-excessive regions (Figure 5a) which would need the necessary water management measures to reduce increased rain-
fall risk if anthropogenic aerosols burden is not controlled. In contrast, a further enhanced deficiency of rainfall driven by
anthropogenic aerosols control (lightly to moderately driven) is also identified to be witnessed over areas of the northern In-
dia (e.g. Punjab and Haryana). While our estimates of aerosol-induced rainfall change corroborate the observational studies
(as also mentioned earlier) showing occurrence of the increased rainfall events during the monsoon seasons in recent years
475 (2018 and 2019) at the southern tip of India (Kerala region), including northeastern India, and areas of Telangana and Andhra
Pradesh, our analysis as presented above further insists the augmented rainfall increase over the region, being governed mainly
by anthropogenic aerosols.

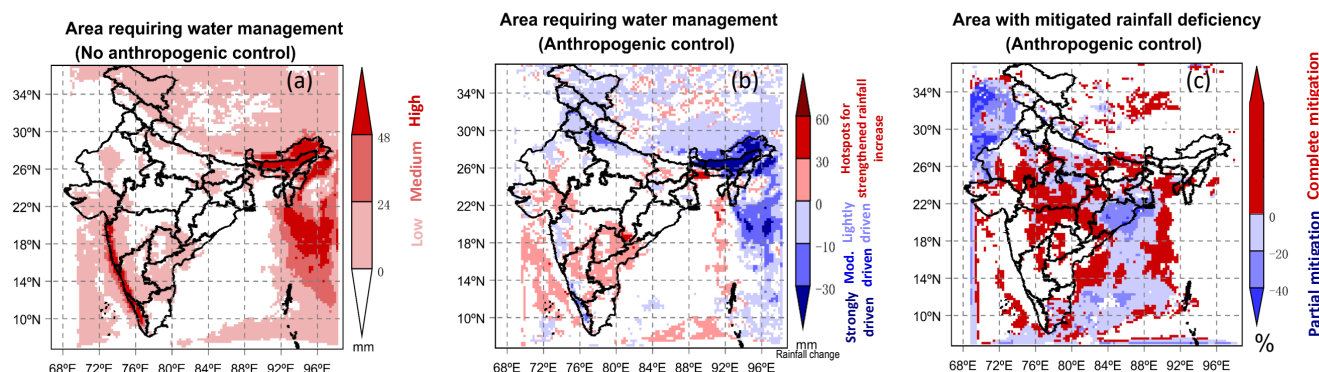


Figure 5. Anthropogenic aerosols control and associated water management. Area requiring (a) degree of water-management (low to high on color scale) for rainfall-excessive areas if no anthropogenic control; (b) water-management driven by anthropogenic control; (c) rainfall deficiency mitigation driven by anthropogenic control. The patches with blue color on color-scale in (b) overlapping with rainfall-excessive areas of (a) (e.g. western coastline, northeastern India) signify mitigated rainfall increase driven by anthropogenic control; and with rainfall-deficient areas of Figure 4d (e.g. northern India over areas of Punjab, Haryana) signify enhanced rainfall-deficiency.

Furthermore, the control of anthropogenic aerosols would also serve to reduce the deficiency in rainfall and areas which would witness mitigation of rainfall deficiency are presented in Figure 5c. The above-mentioned areas are spotted within the identified rainfall-deficient regions of Figure 3d, and corresponds to extracted grids obtained as the difference (%) between dust-induced (or no anthropogenic aerosols, Figure 3f) and all-aerosols induced (Figure 3d) rainfall deficiency. The control of anthropogenic aerosols is thus found leading to a reduction in deficiency by about 20% to 40% over the eastern coast (e.g. West Bengal, Odisha), but that within 20% only over areas of central IGP (e.g. UttarPradesh) and the Bay of Bengal. It however leads to a complete mitigation of rainfall deficiency, e.g. over areas of western India (e.g. Maharashtra, Rajasthan), central India (Chhattisgarh, MadhyaPradesh), and eastern India (Bihar region), that otherwise exhibit all-aerosols-induced rainfall deficiency (Figure 3d).

4 Conclusions

In the present study, we assess the aerosols-driven monsoon-rainfall spatial modulations (weakening and strengthening) over the Indian subcontinent through successfully simulating the measured monsoon-rainfall spatial modulations adequately accounting for aerosol distributions in a fine-resolved ($25 \times 25 \text{ km}^2$) WRF climate model. The monsoon-rainfall spatial modulations are examined in terms of the role of spatial heterogeneity in aerosol species (anthropogenic and dust) radiative perturbations, driving mechanism, including implications of anthropogenic aerosols mitigation on the required water-management measures. In conjunction, the available long-term (1901 to 2014) simulations of monsoon-rainfall from a global aerosol climate model (IPSLCM6A-LR) are also evaluated to present change imposed with aerosols in present years relative to the pre-industrial.



While large values of the modelled AOD due to anthropogenic aerosol (0.3 to 0.6) are predominant over most of India with a specifically higher value over the IGP, eastern coast, and the BoB; these due to dust (as large as 0.3) is seen to be mainly present over northwestern India. The spatially varying AOD due to dust and anthropogenic aerosols are visualized to be spatially concordant to the spatial modulations (strengthening and weakening) in measured monsoon-rainfall (trends and departures), as identified over the IGP and western India, respectively. The observed trend and departures (relative to normal monsoon-rainfall) from measurements indicating the weakening or strengthening of monsoon-rainfall is noted being respectively, 1–7 mm yr⁻² and 20% to 50% in most areas. Aerosol radiative perturbations from ARS show contrasting all-sky aerosol surface radiative effects due to dust and anthropogenic aerosols and a spatially heterogeneous aerosol species-wide radiative perturbations. In contrast to clear-sky aerosol species-wide surface radiative cooling throughout, there is all-sky surface radiative warming over most of mainland India due to dust aerosols, it is surface cooling over most of India but radiative warming along the western coast, central-western area and oceanic regions due to anthropogenic and all-aerosols.

Evaluation of the change in monsoon-rainfall from the long-term simulations (1901 to 2014) from the global climate model (IPSLCM6A-LR) revealed unlike the greenhouse gas warming effect (without aerosol), the change imposed due to aerosol is found to depict the spatial features of observed regional spatial modulations in measured rainfall. The modelled change in rainfall from fine-grid resolved ARS in WRF indicates the monsoon-rainfall as being masked due to anthropogenic aerosols (by 30% to 40%) over most of the Indian subcontinent with the maximum rainfall deficiency (– 48 mm) over the eastern coastal region. In contrast, the monsoon-rainfall is strengthened due to the dust aerosols (> 50%) over most of central and northwestern India, the western and the southern coast (i.e. Kerala region) and at a magnitude of + 51 mm over northwestern India. A striking feature is a concordance of the spatial modulations (weakening and strengthening) in monsoon-rainfall as modelled due to aerosols with the corresponding modulations from measurements. The highest probability density of rainfall deficiency (excessive) values as modelled being about – 10 (+ 14) mm due to anthropogenic (dust) aerosols, including the overall average of the rainfall deficiency (excessive) values across the identified rainfall-deficient (rainfall-excessive) areas, closely matches with the corresponding values from measurements (i.e. departures).

Our study reveals the spatial change in the regional monsoon wind-field dynamics as a potential mechanism explaining the spatially weakening rainfall over the identified areas (e.g. IGP) in the Indian region. The mechanism is mainly driven by aerosol-induced perturbations in regional radiative energy balance, including stronger aerosol radiative forcing contrasts (reversal radiative cooling and warming) between the ocean and land region from anthropogenic than the dust and that from all-sky than the clear-sky. The spatially increasing pattern of monsoon-rainfall over areas such as the western coastal region, central-western and northwestern India) is primarily driven by aerosol-induced all-sky radiative warming and its strengthening due to the dust-induced reduced OLR. Our study, therefore, insists that spatial heterogeneity in aerosol species (anthropogenic, dust, all-aerosols) radiative perturbations primarily drive the regional spatial modulations (weakening and strengthening) in measured monsoon-rainfall over the Indian subcontinent.

Our study shows the control of anthropogenic aerosols would aid in compensating the deficient rainfall or dry spell features by about 20% to 40% over the eastern coast (e.g. West Bengal, Odisha), but that within 20% only over areas of central IGP (e.g. Uttar Pradesh) and the Bay of Bengal. It would however aid in completely mitigating the rainfall deficiency over



areas of western India (e.g. Maharashtra, Rajasthan), central India (Chhattisgarh, MadhyaPradesh), and eastern India (Bihar region). We also identify areas within the identified rainfall-excessive regions with augmented rainfall excessiveness driven by anthropogenic aerosol control (e.g. over Telangana, AndhraPradesh, Karnataka, Gujarat regions) including areas over the Arabian Sea. The above also includes areas with mitigated rainfall excessiveness found to be moderately (e.g. over Kerala region) to strongly driven (e.g. northeastern India) by anthropogenic aerosol control or otherwise needing the necessary water management measures (e.g. to reduce flood risk) due to aerosol-induced increase in rainfall. The present study, therefore, insists policymakers incorporate the implications of anthropogenic emissions and their mitigation in regulating the region-wide water management measures to reduce the societal risks of rainfall deficiency and enhancement (e.g. flood risks) impacting the quality of life of one of the most populous regions in the world.

To our information, this is the first study to successfully simulate aerosol-driven spatial modulations in Indian monsoon rainfall using a fine-resolution regional climate model ($25 \times 25 \text{ km}^2$) that realistically captures both anthropogenic and dust aerosol radiative effects, unlike prior studies (see Section 1). This study also presents the first validated modelled aerosol-induced spatial modulations of monsoon rainfall with model output closely matching the observed rainfall deviations. Our study identifies aerosols as key drivers of persistent regional spatial modulations in monsoon rainfall over the Indian subcontinent. Additionally, we highlight rainfall departures (compared to the normal monsoon) in measured rainfall as a crucial parameter that signals aerosol-induced changes in monsoon patterns.

Our study highlights the spatial changes in the regional monsoon wind fields dynamics and hydrometeorological factors, effectively captured by fine-grid simulations in a regional climate model, as potential governing mechanisms to aerosol-induced changes in monsoon patterns. However, we believe that the magnitude and precision of aerosol-induced responses could be enhanced by incorporating spatially- and temporally fine-resolved global-scale feedback, long-range aerosol transport, and more comprehensive observational validation; these should be considered in future research to improve our understanding of aerosol-monsoon interactions.

Code availability. The Weather Research and Forecasting (WRF) model is available at: <http://www.mmm.ucar.edu/wrf/users/downloads.html>

Data availability. The data in this study are available from the corresponding author upon request (shubha@iitkgp.ac.in).

Author contributions. SS under the supervision of SV conducted the constrained aerosol simulation experiments, AOD and aerosol radiative forcing calculations, and ARS in WRF for aerosol-induced monsoon-rainfall changes and mechanisms, including the PD calculations. SS also compiled the long-term measurement data from IMD and did the PD calculations for measurements and participated with SV in synthesizing and analyzing the results and writing the paper. SV designed and coordinated the study and also wrote the majority of the paper. OB advised throughout in progress and completion of the paper. MKR provided the IMD measurement data and helped in the evaluation of IMD measurements and contributed to the writing of the paper. All authors contributed to the manuscript.



Competing interests. The authors declare that they have no conflict of interest.

Acknowledgements. Simulations were performed in a high-performance computing cluster developed at the Indian Institute of Technology Kharagpur (IIT-KGP) supported through a grant received for the project National Carbonaceous Aerosol Programme–Carbonaceous Aerosol Emissions, Source Apportionment and Climate impacts (NCAP–COALESCE) from the Ministry of Environment, Forest, and Climate Change (14/10/2014-CC (Vo.II)), Govt. of India at the IIT-KGP.

565



References

- Albrecht, B. A.: Aerosols, cloud microphysics, and fractional cloudiness, *Science*, 245, 1227–1230, 1989.
- Asutosh, A. and Vinoj, V.: Role of local absorbing aerosols in modulating Indian summer monsoon rainfall, *Science of The Total Environment*, 910, 168 663, 2024.
- 570 Auffhammer, M., Ramanathan, V., and Vincent, J. R.: Climate change, the monsoon, and rice yield in India, *Climatic change*, 111, 411–424, 2012.
- Barman, N. and Gokhale, S.: Transported aerosols regulate the pre-monsoon rainfall over north-east India: a WRF-Chem modelling study, *Atmospheric Chemistry and Physics*, 23, 6197–6215, 2023.
- Bollasina, M. A., Ming, Y., and Ramaswamy, V.: Anthropogenic aerosols and the weakening of the South Asian summer monsoon, *Science*,
575 334, 502–505, 2011.
- Boucher, O. and Lohmann, U.: The sulfate-CCN-cloud albedo effect, *Tellus B: Chemical and Physical Meteorology*, 47, 281–300, 1995.
- Boucher, O., Balkanski, Y., Hodnebrog, Ø., Myhre, C. L., Myhre, G., Quaas, J., Samset, B. H., Schutgens, N., Stier, P., and Wang, R.: Jury is still out on the radiative forcing by black carbon, *Proceedings of the National Academy of Sciences*, 113, E5092–E5093, 2016.
- Boucher, O., Servonnat, J., Albright, A. L., Aumont, O., Balkanski, Y., Bastrikov, V., Bekki, S., Bonnet, R., Bony, S., Bopp, L., et al.:
580 Presentation and evaluation of the IPSL-CM6A-LR climate model, *Journal of Advances in Modeling Earth Systems*, 12, e2019MS002 010, 2020.
- Charlson, R. J., Schwartz, S. E., Hales, J. M., Cess, R. D., Coakley, J. D., Hansen, J. E., and Hofmann, D. J.: Climate forcing by anthropogenic aerosols, *Science*, 255, 423–430, 1992.
- Cherian, R., Venkataraman, C., Quaas, J., and Ramachandran, S.: GCM simulations of anthropogenic aerosol-induced changes in
585 aerosol extinction, atmospheric heating and precipitation over India, *Journal of Geophysical Research: Atmospheres*, 118, 2938–2955, <https://doi.org/10.1002/jgrd.50298>, 2013.
- Christidis, N. and Stott, P. A.: The Extremely Wet May of 2021 in the United Kingdom, *Bulletin of the American Meteorological Society*, 103, E2912–E2916, 2022.
- Dave, P., Bhushan, M., and Venkataraman, C.: Aerosols cause intraseasonal short-term suppression of Indian monsoon rainfall, *Scientific*
590 *Reports*, 7, 17 347, 2017.
- Debnath, S., Govardhan, G., Saha, S. K., Hazra, A., Pohkrel, S., Jena, C., Kumar, R., and Ghude, S. D.: Impact of dust aerosols on the Indian Summer Monsoon Rainfall on intra-seasonal time-scale, *Atmospheric Environment*, 305, 119 802, 2023.
- Deng, A., Seaman, N. L., and Kain, J. S.: A shallow-convection parameterization for mesoscale models. Part I: submodel description and preliminary applications, *Journal of the Atmospheric Sciences*, 60, 34–56, 2003.
- 595 Deng, A., Gaudet, B., Dudhia, J., and Alapaty, K.: Implementation and evaluation of a new shallow convection scheme in WRF, in: 26th Conf. on Weather Analysis and Forecasting/22nd Conf. on Numerical Weather Prediction, 2014.
- Dumka, U., Kaskaoutis, D., Verma, S., Ningombam, S. S., Kumar, S., and Ghosh, S.: Silver linings in the dark clouds of COVID-19: improvement of air quality over India and Delhi metropolitan area from measurements and WRF-CHIMERE model simulations, *Atmospheric Pollution Research*, 12, 225–242, 2021.
- 600 Eichel, C., Krämer, M., Schütz, L., and Wurzler, S.: The water-soluble fraction of atmospheric aerosol particles and its influence on cloud microphysics, *Journal of Geophysical Research: Atmospheres*, 101, 29 499–29 510, 1996.



- Fadnavis, S., Roy, C., Sabin, T., Ayantika, D., and Ashok, K.: Potential modulations of pre-monsoon aerosols during El Niño: impact on Indian summer monsoon, *Climate Dynamics*, 49, 2279–2290, 2017.
- Forster, P., Ramaswamy, V., Artaxo, P., Berntsen, T., Betts, R., Fahey, D. W., Haywood, J., Lean, J., Lowe, D. C., Myhre, G., Nganga, J., Prinn, R., Raga, G., Schulz, M., and Dorland, R. V.: Changes in Atmospheric Constituents and in Radiative Forcing, in *Climate Change 2007: The Physical Science Basis. Contribution of Working Group I to the Fourth Assessment Report of the Intergovernmental Panel on Climate Change* edited by Solomon, S., D. Qin, M. Manning, Z. Chen, M. Marquis, K.B. Averyt, M. Tignor and H.L. Miller, Cambridge University Press, Newyork, 186–217, 2007.
- Gadgil, S. and Sajani, S.: Monsoon precipitation in the AMIP runs, *Climate Dynamics*, 14, 659–689, 1998.
- 605 Ganguly, D., Rasch, P. J., Wang, H., and Yoon, J.: Fast and slow responses of the South Asian monsoon system to anthropogenic aerosols, *Geophysical Research Letters*, 39, 1–5, <https://doi.org/10.1029/2012GL053043>, 2012a.
- Ghosh, S. and Verma, S.: Estimates of spatially and temporally resolved constrained organic matter and sulfur dioxide emissions over the Indian region through the strategic source constraints modelling, *Atmospheric Research*, 282, 106 504, 2023.
- Ghosh, S., Vittal, H., Sharma, T., Karmakar, S., Kasiviswanathan, K., Dhanesh, Y., Sudheer, K., and Gunthe, S.: Indian summer monsoon rainfall: implications of contrasting trends in the spatial variability of means and extremes, *PLoS One*, 11, e0158 670, 2016.
- 615 Ghosh, S., Verma, S., Kuttippurath, J., and Menut, L.: Wintertime direct radiative effects due to black carbon (BC) over the Indo-Gangetic Plain as modelled with new BC emission inventories in CHIMERE, *Atmospheric Chemistry and Physics*, 21, 7671–7694, 2021.
- Haupt, S. E., Kosovic, B., Jensen, T., Cowie, J., Jimenez, P., and Wiener, G.: Comparing and integrating solar forecasting techniques, in: 2016 IEEE 43rd Photovoltaic Specialists Conference (PVSC), pp. 0953–0955, IEEE, 2016.
- 620 Herbert, R., Wilcox, L. J., Joshi, M., Highwood, E., and Frame, D.: Nonlinear response of Asian summer monsoon precipitation to emission reductions in South and East Asia, *Environmental Research Letters*, 17, 014 005, 2021.
- Hourdin, F. and Armengaud, A.: The use of finite-volume methods for atmospheric advection of trace species. Part I: test of various formulations in a general circulation model, *Monthly Weather Review*, 127, 822–837, 1999.
- Iacono, M. J., Delamere, J. S., Mlawer, E. J., Shephard, M. W., Clough, S. A., and Collins, W. D.: Radiative forcing by long-lived greenhouse gases: calculations with the AER radiative transfer models, *Journal of Geophysical Research: Atmospheres*, 113, 2008.
- 625 Indian Meteorological Department: Indian Meteorological Department, <https://mausam.imd.gov.in/responsive/monsooninformation.php>, accessed: 20-07-2023, 2019.
- Jimenez, P. A., Hacker, J. P., Dudhia, J., Haupt, S. E., Ruiz-Arias, J. A., Gueymard, C. A., Thompson, G., Eidhammer, T., and Deng, A.: WRF-Solar: Description and clear-sky assessment of an augmented NWP model for solar power prediction, *Bulletin of the American Meteorological Society*, 97, 1249–1264, 2016.
- 630 Jin, Q., Yang, Z.-L., and Wei, J.: Seasonal responses of Indian summer monsoon to dust aerosols in the Middle East, India, and China, *Journal of Climate*, 29, 6329–6349, 2016.
- Katzenberger, A., Schewe, J., Pongratz, J., and Levermann, A.: Robust increase of Indian monsoon rainfall and its variability under future warming in CMIP6 models, *Earth System Dynamics*, 12, 367–386, 2021.
- 635 Kripalani, R., Ha, K.-J., Ho, C.-H., Oh, J.-H., Preethi, B., Mujumdar, M., and Prabhu, A.: Erratic Asian summer monsoon 2020: COVID-19 lockdown initiatives possible cause for these episodes?, *Climate dynamics*, 59, 1339–1352, 2022.
- Kumar, D. B. and Verma, S.: Potential emission flux to aerosol pollutants over Bengal Gangetic plain through combined trajectory clustering and aerosol source fields analysis, *Atmospheric Research*, 178, 415–425, 2016.



- Kumar, D. B., Verma, S., Boucher, O., and Wang, R.: Constrained simulation of aerosol species and sources during pre-monsoon season over
640 the Indian subcontinent, *Atmospheric Research*, 214, 91–108, 2018.
- Lau, K. M., Kim, M. K., and Kim, K. M.: Asian summer monsoon anomalies induced by aerosol direct forcing: the role of the Tibetan
Plateau, *Climate Dynamics*, 26, 855–864, 2006.
- Lau, W. K., Kim, K.-M., Shi, J.-J., Matsui, T., Chin, M., Tan, Q., Peters-Lidard, C., and Tao, W.: Impacts of aerosol–monsoon interaction on
rainfall and circulation over Northern India and the Himalaya Foothills, *Climate Dynamics*, 49, 1945–1960, 2017.
- 645 Lawrence, M. G. and Lelieveld, J.: Atmospheric pollutant outflow from Southern Asia: a review, *Atmospheric Chemistry and Physics*, 10,
11 017–11 096, <https://doi.org/10.5194/acp-10-11017-2010>, 2010.
- Liou, K. N.: *An Introduction to Atmospheric Radiation*, Academic Press, San Diego, Calif, PP. 392, 1980.
- Lobell, D. B., Schlenker, W., and Costa-Roberts, J.: Climate trends and global crop production since 1980, *Science*, 333, 616–620, 2011.
- Menon, S., Hansen, J., Nazarenko, L., and Luo, Y.: Climate effects of black carbon aerosols in China and India, *Science*, 297, 2250–2253,
650 2002.
- O’Neill, B. C., Tebaldi, C., Van Vuuren, D. P., Eyring, V., Friedlingstein, P., Hurtt, G., Knutti, R., Kriegler, E., Lamarque, J.-F., Lowe, J.,
et al.: The scenario model intercomparison project (ScenarioMIP) for CMIP6, *Geoscientific Model Development*, 9, 3461–3482, 2016.
- Parthasarathy, B., Munot, A., and Kothawale, D.: All-India monthly and seasonal rainfall series: 1871–1993, *Theoretical and Applied Cli-
matology*, 49, 217–224, 1994.
- 655 Persad, G. G., Samset, B. H., and Wilcox, L. J.: Aerosols must be included in climate risk assessments, *Nature*, 611, 662–664, 2022.
- Rajendran, K., Surendran, S., Varghese, S. J., and Sathyanath, A.: Simulation of Indian summer monsoon rainfall, interannual variability and
teleconnections: evaluation of CMIP6 models, *Climate Dynamics*, 58, 2693–2723, 2022.
- Rajesh, P. and Goswami, B.: Climate change and potential demise of the Indian deserts, *Earth’s Future*, 11, e2022EF003 459, 2023.
- Ramanathan, V., Chung, C., Kim, D., Bettge, T., Buja, L., Kiehl, J., Washington, W., Fu, Q., Sikka, D., and Wild, M.: Atmospheric brown
660 clouds: Impacts on South Asian climate and hydrological cycle, *Proceedings of the National Academy of Sciences of the United States of
America*, 102, 5326–5333, 2005.
- Risser, M. D., Collins, W. D., Wehner, M. F., O’Brien, T. A., Huang, H., and Ullrich, P. A.: Anthropogenic aerosols mask increases in US
rainfall by greenhouse gases, *Nature Communications*, 15, 1318, 2024.
- Roxy, M. K., Ghosh, S., Pathak, A., Athulya, R., Mujumdar, M., Murtugudde, R., Terray, P., and Rajeevan, M.: A threefold rise in widespread
665 extreme rain events over Central India, *Nature communications*, 8, 1–11, 2017.
- Ruiz-Arias, J. A., Dudhia, J., Santos-Alamillos, F. J., and Pozo-Vázquez, D.: Surface clear-sky shortwave radiative closure intercomparisons
in the Weather Research and Forecasting model, *Journal of Geophysical Research: Atmospheres*, 118, 9901–9913, 2013.
- Sajani, S., Moorthy, K. K., Rajendran, K., and Nanjundiah, R. S.: Monsoon sensitivity to aerosol direct radiative forcing in the community
atmosphere model, *Journal of Earth System Science*, 121, 867–889, 2012.
- 670 Samset, B. H., Lund, M. T., Bollasina, M., Myhre, G., and Wilcox, L.: Emerging Asian aerosol patterns, *Nature Geoscience*, 12, 582–584,
2019.
- Seth, A., Giannini, A., Rojas, M., Rauscher, S. A., Bordoni, S., Singh, D., and Camargo, S. J.: Monsoon responses to climate
changes—connecting past, present and future, *Current Climate Change Reports*, 5, 63–79, 2019.
- Shawki, D., Voulgarakis, A., Chakraborty, A., Kasoar, M., and Srinivasan, J.: The South Asian monsoon response to remote aerosols: global
675 and regional mechanisms, *Journal of Geophysical Research: Atmospheres*, 123, 11–585, 2018.



- Singh, P., Gnanaseelan, C., and Chowdary, J.: North-East monsoon rainfall extremes over the southern peninsular India and their association with El Niño, *Dynamics of Atmospheres and Oceans*, 80, 1–11, 2017.
- Skliris, N., Marsh, R., Haigh, I. D., Wood, M., Hirschi, J., Darby, S., Quynh, N. P., and Hung, N. N.: Drivers of rainfall trends in and around Mainland Southeast Asia, *Frontiers in Climate*, 4, 926 568, 2022.
- 680 Stier, P., van den Heever, S. C., Christensen, M. W., Gryspeerdt, E., Dagan, G., Saleeby, S. M., Bollasina, M., Donner, L., Emanuel, K., Ekman, A. M., et al.: Multifaceted aerosol effects on precipitation, *Nature Geoscience*, 17, 719–732, 2024.
- Stromatas, S., Turquety, S., Menut, L., Chepfer, H., Pere, J.-C., Cesana, G., and Bessagnet, B.: Lidar signal simulation for the evaluation of aerosols in chemistry transport models, *Geoscientific Model Development*, 5, 1543–1564, 2012.
- Thompson, G. and Eidhammer, T.: A study of aerosol impacts on clouds and precipitation development in a large winter cyclone, *Journal of*
- 685 *the Atmospheric Sciences*, 71, 3636–3658, 2014.
- Twomey, S. et al.: Pollution and the planetary albedo, *Atmospheric Environment*, 8, 1251–1256, 1974.
- Verma, S., Venkataraman, C., and Boucher, O.: Origin of surface and columnar INDOEX aerosols using source- and region-tagged emissions transport in a general circulation model, *J. Geophys. Res.*, 113, D24211, <https://doi.org/10.1029/2007JD009538>, 2008.
- Verma, S., Ghosh, S., Boucher, O., Wang, R., and Menut, L.: Black carbon health impacts in the Indo-Gangetic plain: exposures, risks, and
- 690 mitigation, *Science Advances*, 8, eabo4093, 2022.
- Vijaykumar, P., Abhilash, S., Sreenath, A., Athira, U., Mohanakumar, K., Mapes, B., Chakrapani, B., Sahai, A., Niyas, T., and Sreejith, O.: Kerala floods in consecutive years-Its association with mesoscale cloudburst and structural changes in monsoon clouds over the West coast of India, *Weather and Climate Extremes*, p. 100339, 2021.
- Vinoj, V., Rasch, P. J., Wang, H., Yoon, J.-H., Ma, P.-L., Landu, K., and Singh, B.: Short-term modulation of Indian summer monsoon rainfall by West Asian dust, *Nature Geoscience*, 7, 308, 2014.
- 695 Wang, F., Zhao, X., Gerlein-Safdi, C., Mu, Y., Wang, D., and Lu, Q.: Global sources, emissions, transport and deposition of dust and sand and their effects on the climate and environment: a review, *Frontiers of Environmental Science & Engineering*, 11, 1–9, 2017.
- Zhang, D.-L.: Rapid urbanization and more extreme rainfall events, *Science Bulletin*, 65, 516–518, 2020.